

Bone Marrow Stromal Cell Transplantation Enhances Recovery of Local Glucose Metabolism After Cerebral Infarction in Rats: A Serial ^{18}F -FDG PET Study

Michiyuki Miyamoto¹, Satoshi Kuroda¹, Songji Zhao², Keiichi Magota³, Hideo Shichinohe¹, Kiyohiro Houkin¹, Yuji Kuge⁴, and Nagara Tamaki³

¹Department of Neurosurgery, Hokkaido University Graduate School of Medicine, Sapporo, Japan; ²Department of Tracer Kinetics and Bioanalysis, Hokkaido University Graduate School of Medicine, Sapporo, Japan; ³Department of Nuclear Medicine, Hokkaido University Graduate School of Medicine, Sapporo, Japan; and ⁴Central Institute of Isotope Science, Hokkaido University, Sapporo, Japan

This study aimed to assess whether ^{18}F -FDG PET could serially monitor the beneficial effects of bone marrow stromal cells (BMSC) on cerebral glucose metabolism when transplanted into the infarct brain of rats. **Methods:** The BMSC from green fluorescent protein transgenic rats or vehicle was stereotactically transplanted into the ipsilateral striatum at 7 d after permanent middle cerebral artery occlusion of rats. Local glucose metabolism was semiquantitatively measured at 6 and 35 d after ischemia using ^{18}F -FDG PET. Motor function was serially evaluated throughout the experiments. At 35 d after ischemia, immunohistochemistry was performed to evaluate the phenotype of BMSC and their effects on the expression of brain-type glucose transporters. **Results:** BMSC transplantation not only enhanced functional recovery but also promoted the recovery of glucose utilization in the periinfarct area when stereotactically transplanted at 1 wk after ischemia. The engrafted cells were widely distributed, and most expressed a neuron-specific protein, NeuN. BMSC transplantation also prevented the pathologic upregulation of glucose transporters in the periinfarct neocortex. **Conclusion:** The present findings strongly suggest that the BMSC may enhance functional recovery by promoting the recovery of local glucose metabolism in the periinfarct area when directly transplanted into the infarct brain at clinically relevant timing. The BMSC also inhibit the pathologic upregulation of brain-isoform glucose transporters type 1 and 3. ^{18}F -FDG PET may be a valuable modality to scientifically prove the beneficial effects of BMSC transplantation on the host brain in clinical situations.

Key Words: cerebral infarct; bone marrow stromal cell; transplantation; ^{18}F -FDG; PET

J Nucl Med 2013; 54:145–150

DOI: 10.2967/jnumed.112.109017

Recent works have clearly shown that the bone marrow stromal cells (BMSCs) may promote functional recovery after various kinds of central nervous system (CNS) disorders, including ischemic stroke. BMSCs may contribute to functional recovery through multiple mechanisms. They have the capacity to differentiate into the neural cells (1–4). Alternatively, they support the host neurons and promote axonal regeneration by releasing neuroprotective or neurotrophic factors such as brain-derived neurotrophic factor (5–8). The BMSCs are far more accessible than other stem cells without posing ethical or immunologic difficulties, because they can be obtained from the patients themselves and they have no tumorigenesis (9). The results from preclinical testing are promising. Preliminary clinical trials have already been conducted.

As was recently pointed out, however, there are several concerns to be resolved before the clinical application of BMSCs for CNS disorders. The issues include the development of imaging techniques to track the engrafted cells and to monitor the response of the host CNS (10–13). These techniques would enable validation of the therapeutic benefits of BMSC transplantation without any bias. Other recent studies have suggested that MRI and optical imaging might provide useful information on the engraftment of BMSCs in the host CNS (14–18). However, there are few studies that indicate the utility of an imaging technique to monitor the response of the host CNS after cell therapy (19–21).

On the basis of these considerations, therefore, this study aimed to assess whether ^{18}F -FDG PET could serially monitor the effects of BMSC transplantation on cerebral glucose metabolism when BMSCs are stereotactically transplanted into the infarct brain of rats.

MATERIALS AND METHODS

BMSC Preparation

All animal experiments were approved by the Animal Studies Ethical Committee of Hokkaido University Graduate School of

Received May 17, 2012; revision accepted Aug. 6, 2012.

For correspondence or reprints contact: Satoshi Kuroda, Department of Neurosurgery, Hokkaido University Graduate School of Medicine, North 15 West 7, Kita-ku, Sapporo 060-8638, Japan.

E-mail: skuroda@med.hokudai.ac.jp

Published online Nov. 30, 2012.

COPYRIGHT © 2013 by the Society of Nuclear Medicine and Molecular Imaging, Inc.

Medicine. The BMSCs were isolated under sterile conditions from male 8-wk-old transgenic rats expressing enhanced green fluorescent protein (GFP) (Japan SLC Inc.) and were cultured as previously reported (14,18,22,23). The cells were passed 3 times for subsequent experiments.

Permanent Middle Cerebral Artery (MCA) Occlusion Model

Male 8-wk-old Sprague–Dawley rats were purchased from CLEA Japan Inc. Permanent MCA occlusion was induced, as described previously (14,18,22,23). Briefly, anesthesia was induced by 4.0% isoflurane in N₂O/O₂ (70:30) and was maintained with 2.0% isoflurane in N₂O/O₂ (70:30). Core temperature was maintained between 36.5°C and 37.0°C through the procedures. The bilateral common carotid arteries were exposed through a ventral midline incision of the neck. Then, a 1.5-cm vertical skin incision was performed between the right eye and ear. The temporal muscle was scraped from temporal bone, and a 5 × 5 mm temporal craniotomy was performed, using a small dental drill. To prevent cerebrospinal fluid leakage, the dura mater was carefully kept intact, and the right MCA was ligated using a 10-0 nylon thread through the dura mater. Then, the cranial window was closed with the temporal bone flap. The temporal muscle and skin were sutured with 4-0 nylon threads. Subsequently, the bilateral common carotid arteries were occluded by surgical microclips for 1 h. Only the animals that circled toward the paretic side after surgery were included in this study (24).

BMSC Transplantation

The GFP-expressing BMSC or vehicle was stereotactically transplanted into the ipsilateral striatum at 7 d after ischemia ($n = 9$ in each group), as reported previously (14,18,20,22,23,25). Briefly, a burr hole was made 3 mm to the right of the bregma. A Hamilton syringe was inserted 5 mm into the brain parenchyma from the surface of the dura mater. The BMSCs were suspended in phosphate-buffered solution, and 10 μ L of cell suspension (1×10^6 cells) were introduced into the striatum. In the vehicle group, 10 μ L of only the phosphate-buffered solution were introduced, in the same fashion as in the BMSC group.

Behavioral Test

The motor function of the animals was assessed before and at 7, 14, 21, 28, and 35 d after the onset of ischemia, using a rotarod treadmill (model MK-630; Muromachi Kikai Co.). The test has been proven to have high interrater and interlaboratory reliability (26). The rotarod was set to the acceleration mode of 4–40 rpm for 5 min. All animals were trained for 3 d before the study. The maximum time that the animal stayed on the rotarod was recorded for each performance, as described previously (22,23).

¹⁸F-FDG PET

Cerebral glucose metabolism was semiquantitatively measured, using a high-resolution small-animal imaging system (Inveon PET/CT; Siemens Medical Solutions). The PET component consists of $1.5 \times 1.5 \times 10$ mm lutetium oxyorthosilicate crystal elements with a ring diameter of 16.1 cm, providing a 10-cm transaxial and a 12.7-cm axial field of view (27–29).

PET measurements were repeated in each animal at 6 and 35 d after the onset of permanent MCA occlusion—that is, 1 d before and 28 d after stereotactic BMSC transplantation. The animals were kept fasting for 12 h before PET. They were held still without anesthesia, and approximately 37 MBq of ¹⁸F-FDG were injected via the tail vein. They were returned to their cage and were allowed to

move freely for 60 min. Subsequently, they were anesthetized with 2.0% isoflurane in air and were scanned by PET for 30 min. The acquired data were assumed to represent glucose utilization in the brain tissue, because 45 min would be enough to wash out the non-metabolized ¹⁸F-FDG from the brain tissue and to reduce the radioactivity of ¹⁸F-FDG in the circulating blood. A CT scan was also obtained for attenuation correction. The core temperature of the animals was maintained as a constant between 37.5°C and 38.5°C throughout the examination, using a heating pad.

The acquired data were reconstructed, using filtered back-projection and a maximum a posteriori algorithm, as reported previously (28,30,31). Attenuation and scatter corrections were performed, using a CT-based method. The spatial resolution was 1.63 mm in full width at half maximum for the filtered back-projection method and 1.05 mm in full width at half maximum for the maximum a posteriori method. The former was used to quantify the radioactivity, and the latter was used for visual observations. Regions of the interest (ROIs) were symmetrically placed in the dorsal neocortex and striatum, and the ratio of ipsilateral to contralateral radioactivity was calculated, using IDL (Research Systems) and ASIPro (Concorde Microsystems).

Histologic Analysis

At 4 wk after transplantation, the animals were deeply anesthetized with 4.0% isoflurane in N₂O/O₂ (70:30) and transcardially perfused. The brain was removed, and 4- μ m-thick coronal sections were prepared for subsequent analysis. Double fluorescence immunohistochemistry was performed, as reported previously (14,18,22,23). Briefly, each section was treated with primary antibody against glial fibrillary acidic protein (GFAP) (mouse monoclonal, 1:500 dilution; BD Pharmingen) or NeuN (mouse monoclonal, 1:100 dilution; Millipore) and labeled with Alexa Fluor 594 (Molecular Probes Inc.). Subsequently, the sections were incubated with primary antibody against GFP (mouse monoclonal, 1:100 dilution; Santa Cruz) tagged with Zenon Alexa Fluor 488 (Molecular Probes Inc.). Three ROIs (450 × 550 μ m) were symmetrically placed in the dorsal neocortex adjacent to the cerebral infarct. The percentages of the cells that were doubly positive for GFP and NeuN to the GFP-positive cells were calculated.

Furthermore, the sections were treated with primary antibody against glucose transporter 1 (GLUT1; mouse monoclonal, 1:200 dilution; Abcam) or glucose transporter 3 (GLUT3; mouse monoclonal, 1:100 dilution; Santa Cruz) at room temperature for 1 h and then labeled with Alexa Fluor 594 at room temperature for 1 h. Subsequently, the sections were incubated with primary antibody against NeuN tagged with Zenon Alexa Fluor 488 at room temperature for 1 h. To analyze the density of the GLUT1-positive microvasculature, the ROIs (900 × 1,100 μ m) were symmetrically placed in the dorsal neocortex. Then, the area of GLUT1-positive blood vessels in each ROI was quantified, using the image analyzing system (Image J) (32). Briefly, the red fluorescence signal emitted from microvasculature stained with anti-GLUT1 antibody was binarized (as black signal on white background) and quantified as the GLUT1-positive vascular fraction, and then the area of the GLUT1-positive blood vessels in each ROI was presented as the percentage of GLUT1-positive area to the whole area of ROI. Finally, to assess the effect of BMSC transplantation on GLUT3 expression, the ROIs (450 × 550 μ m) were symmetrically placed in the dorsal neocortex. The number of cells positive for GLUT3 was counted in each ROI.

Statistical Analysis

All data were expressed as mean \pm SD. Continuous data were compared by Student *t* test. *P* values of less than 0.05 were considered statistically significant.

RESULTS

Effects of BMSC Transplantation on Functional Recovery

All animals exhibited a severe neurologic deficit at 6 d after ischemia. There was no significant difference in motor function between the vehicle- and BMSC-transplanted animals. Subsequently, the vehicle-transplanted animals did not show any significant improvement of motor function. In contrast, motor function in the BMSC-transplanted animals significantly recovered at 4 wk after BMSC transplantation ($P = 0.038$, Fig. 1).

Effects of BMSC Transplantation on Glucose Metabolism

Using ^{18}F -FDG PET, we semiquantitatively evaluated glucose metabolism at 6 and 35 d after ischemia. As shown in Figure 2, glucose utilization was markedly decreased in the ipsilateral neocortex at 6 d after ischemia. In the vehicle-transplanted animals, glucose utilization improved to some extent in the periinfarct neocortex at 35 d after ischemia (Figs. 2A and 2B). However, BMSC transplantation significantly accelerated the recovery in the periinfarct neocortex at the same time point (Figs. 2C and 2D).

The ipsilateral-to-contralateral ratio of local glucose utilization in the dorsal neocortex significantly increased from $72.5\% \pm 4.2\%$ to $78.7\% \pm 4.0\%$ in the vehicle-treated group ($P = 0.0046$, Fig. 3). However, the value more pronouncedly increased from $72.7\% \pm 4.4\%$ to $87.7\% \pm 5.3\%$ in the BMSC-treated group ($P < 0.001$). The ratio was significantly higher in the BMSC-treated group than in the vehicle-treated

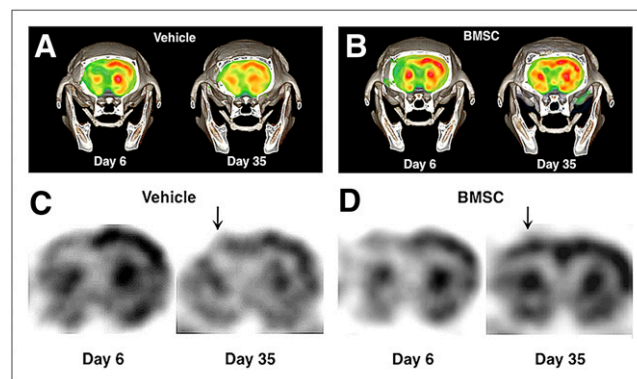


FIGURE 2. Representative findings of ^{18}F -FDG PET at 6 and 35 d after ischemia. Color (A) and black-and-white (C) images of vehicle-transplanted animals. Color (B) and black-and-white (D) images of BMSC-transplanted rats. There was significant increase in local glucose metabolism in periinfarct neocortex (arrows).

group at 35 d after ischemia ($P < 0.001$). These findings were not observed in the striatum.

Histologic Analysis

Representative results of fluorescence immunohistochemistry in the BMSC-transplanted animals are shown in Figure 4. Many of the GFP-expressing cells were extensively distributed in the dorsal neocortex adjacent to the cerebral infarct at 4 wk after transplantation (14.2 ± 7.6 cells/mm 2). Most of the cells ($86.0\% \pm 26.1\%$) were also positive for NeuN. The GFP-expressing cells in the ipsilateral hippocampus were also positive for NeuN. Some GFP-positive cells also expressed GFAP in the periinfarct areas.

The area of GLUT1-positive vascular fraction was significantly higher in the ipsilateral neocortex than in the contralateral neocortex of the vehicle-transplanted animals ($2.62\% \pm 0.43\%$ and $2.21\% \pm 0.67\%$, respectively) ($P = 0.023$). On the other hand, there was no significant difference between the ipsi- and contralateral neocortex in the

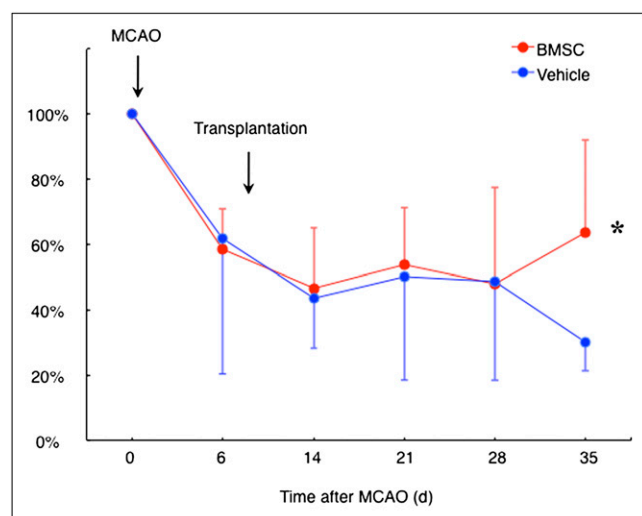


FIGURE 1. Rotarod treadmill performance. Line shows temporal profile of functional recovery in vehicle- and BMSC-transplanted rats subjected to permanent MCA occlusion (MCAO). * $P < 0.05$.

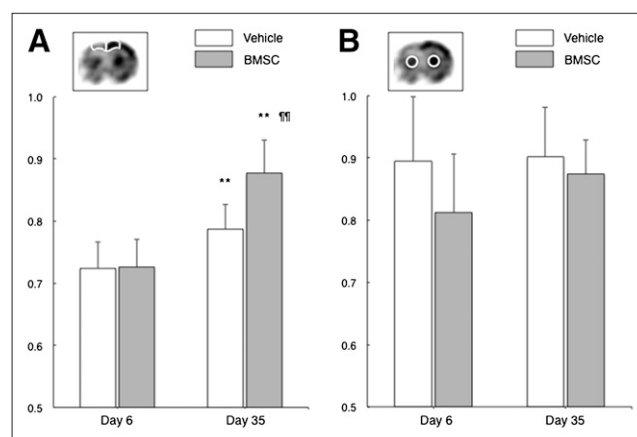


FIGURE 3. Bar graphs show ipsilateral-to-contralateral ratio of cerebral glucose utilization in dorsal neocortex adjacent to cerebral infarct (A) and striatum (B). ** $P < 0.01$ (day 6 vs. day 35). ¶ $P < 0.01$ (vehicle vs. BMSC).

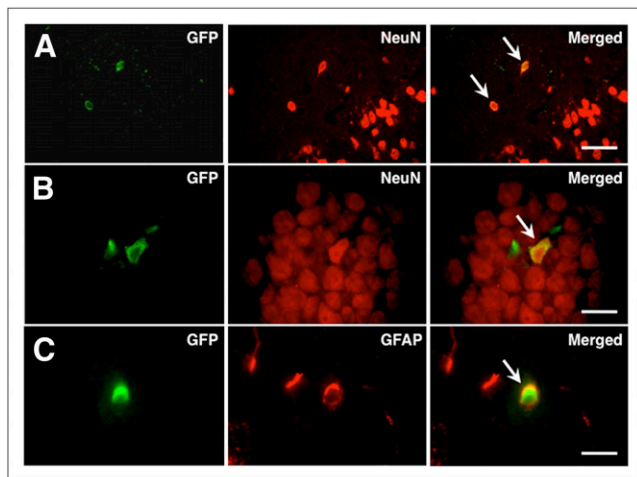


FIGURE 4. Photomicrographs of double immunohistochemistry in periinfarct neocortex (A and C) and ipsilateral hippocampus (B). Most GFP-positive cells (green) were also positive for NeuN (red; arrows in A and B) and GFAP (red; arrow in C). Scale bars = 100 μ m (A) and 50 μ m (B and C).

BMSC-transplanted animals ($2.05\% \pm 0.34\%$ and $2.32\% \pm 0.44\%$, respectively) (Fig. 5).

A certain subgroup of neurons was positive for GLUT3 in the normal neocortex (Fig. 6A). The GLUT3-positive cells significantly increased in the ipsilateral dorsal neocortex of the vehicle-transplanted animals (Figs. 6B and 6C). The number of GLUT3-positive cells was significantly higher in the ipsilateral neocortex than in the contralateral neocortex of the vehicle-transplanted animals (67.2 ± 19.2 and 56.8 ± 20.3 , respectively) ($P = 0.034$). On the other hand, there was no significant difference between the ipsi- and contralateral neocortex in the BMSC-transplanted animals (48.9 ± 19.3 and 55.6 ± 16.1 , respectively).

DISCUSSION

Using a PET/CT apparatus designed for small animals, this study clearly demonstrates that the BMSCs not only enhance functional recovery but also promote the recovery of glucose utilization in the periinfarct area after ischemic stroke, when stereotactically transplanted at 1 wk after ische-

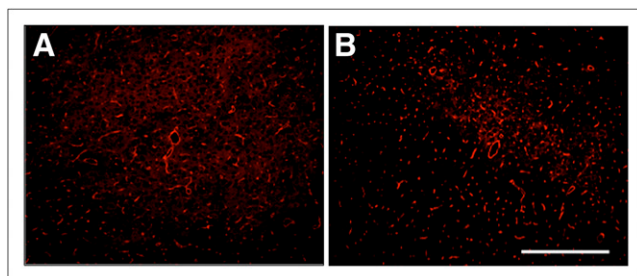


FIGURE 5. Photomicrographs of fluorescence immunohistochemistry against GLUT1 in periinfarct neocortex of vehicle- (A) and BMSC-transplanted animals (B). Scale bars = 200 μ m.

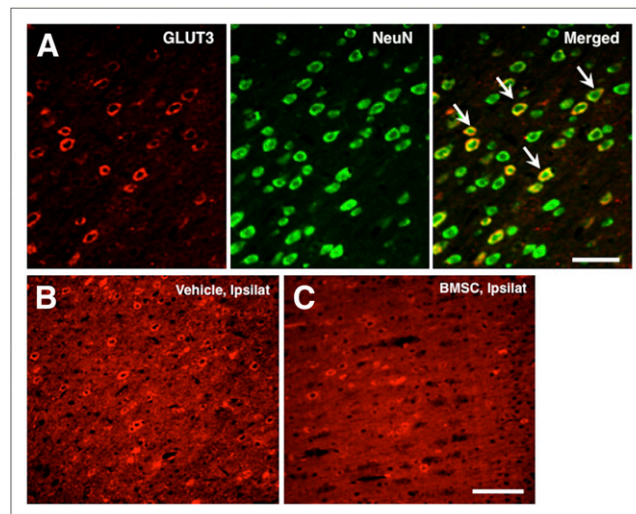


FIGURE 6. (A) Photomicrographs of double immunohistochemistry against GLUT3 (red) and NeuN (green) in contralateral neocortex of vehicle-transplanted animals. Subgroup of NeuN-positive cells was also positive for GLUT3. Scale bars = 100 μ m. (B and C) Photomicrographs of fluorescence immunohistochemistry against GLUT3 in ipsilateral neocortex of vehicle- (A) and BMSC-transplanted animals (B). Scale bars = 200 μ m. Ipsilat = ipsilateral neocortex.

mia. The cells are widely engrafted, and most express NeuN, suggesting that they contribute to metabolic and functional recovery, at least in part, by replacing the damaged neural cells around cerebral infarct.

Previously, the application of ^{18}F -FDG PET has been limited to large laboratory animals such as nonhuman primates to monitor cerebral glucose utilization, because of the limited resolution of the PET scanner. However, the recent improvement in scanner technology has made it possible to measure cerebral glucose utilization in rodent brains. Moore et al. reported that ^{18}F -FDG PET of rats is quantitative, reproducible, and sensitive to metabolic changes (33). Shimoji et al. reached similar conclusions (34). However, the quantification of cerebral glucose utilization in small animals may have some problems. For example, abundant blood sampling may affect their physiologic conditions, and their small brains may cause partial-volume effects (33,34). In this study, therefore, we evaluated cerebral glucose utilization by calculating the ipsilateral-to-contralateral ratio in each ROI. Furthermore, data sampling was performed under anesthesia with isoflurane in this study. However, the animals received the ^{18}F -FDG injection without anesthesia and were allowed to move freely in their cage for 60 min after injection, suggesting that ^{18}F -FDG uptake was essentially complete (35).

BMSCs promote functional recovery through multiple mechanisms, including their neural differentiation and release of neuroprotective or neurotrophic factors. The facts may explain why therapeutic effects are observed at 4 wk after BMSC transplantation (Fig. 1). However, current knowledge about cell therapy for ischemic stroke is based principally on histologic findings, and it is still unclear how

the engrafted BMSCs restore the lost neural function. Thus, a considerable gap exists between histologic findings and the understanding of functional recovery. Only a few studies have been run to elucidate the effect of BMSC transplantation on brain function. Using an autoradiography technique, Mori et al. found that BMSC transplantation significantly improved glucose metabolism in the thalamus and barrel cortex in response to whisker stimulation after neocortical freezing injury (19). We also showed that BMSC transplantation significantly improved the binding potential of ^{125}I -iomazenil, a radioactive ligand selective for the central type of benzodiazepine receptor, in the periinfarct area. Simultaneously, the engrafted BMSCs expressed the marker protein specific for γ -aminobutyric acid receptor in the periinfarct area (20). Similar results were obtained in the rodent model of spinal cord injury (21). These results strongly indicate the utility of nuclear imaging to evaluate the beneficial effects of cell therapy. However, autoradiography allows observation at only 1 time point using postmortem study and cannot evaluate serial changes of brain function in living animals. Therefore, we have used a PET/CT apparatus to longitudinally and noninvasively monitor the changes in brain metabolism in each animal in this study.

Another impact of this study is the fact that BMSC transplantation significantly prevents the pathologic upregulation of glucose transporter in the periinfarct neocortex. Glucose transporters are the facilitative Na^+ -independent sugar transporters and have 13 isoforms (36). Brain tissue mainly has GLUT1 and GLUT3, which are localized in the endothelial cells and neurons, respectively (37,38). Previous studies have shown that these glucose transporters are upregulated under conditions of cerebral ischemia (39). Indeed, the density of both GLUT1 and GLUT3 is significantly increased in the periinfarct neocortex of the vehicle-transplanted animals, suggesting the self-adaptation to protect the brain by ensuring the glucose delivery to the tissue. However, the BMSCs significantly suppress their upregulation by improving glucose utilization in the periinfarct neocortex. The underlying mechanisms through which the BMSCs suppress the upregulation of GLUT1 and GLUT3 is unclear, but it is most likely that the engrafted cells may play a key role in maintaining glucose transporter function by replacing the neural cells or releasing neuroprotective factors. However, further studies are necessary to elucidate this issue.

Furthermore, this study strongly suggests that ^{18}F -FDG PET may be a promising modality to assess the therapeutic benefits of cell therapy for ischemic stroke without bias. As mentioned, most previous clinical trials of cell therapy for CNS disorders have evaluated therapeutic efficacy by assessing functional outcome. On the basis of historical considerations of the development of neuroprotective drugs, however, it would be essential to establish another surrogate biomarker to bridge the still-existing gap between preclinical studies and clinical testing (12). From this viewpoint, ^{18}F -FDG PET may be useful to visualize the therapeutic efficacy of cell therapy and functional outcome. In this study, the effect

of BMSC transplantation on infarct core tissue is unknown, because the tissue markedly shrinks at 5 wk after ischemia.

CONCLUSION

The present findings strongly suggest that the BMSCs may enhance functional recovery by promoting the restoration of local glucose metabolism in the periinfarct area when directly transplanted into the infarcted brain with clinically relevant timing. The BMSCs also inhibit pathologic upregulation of brain-isoform glucose transporters GLUT1 and GLUT3. ^{18}F -FDG PET is the candidate of choice for valuable modalities to scientifically prove the beneficial effects of BMSC transplantation on the host brain in clinical situations.

DISCLOSURE

The costs of publication of this article were defrayed in part by the payment of page charges. Therefore, and solely to indicate this fact, this article is hereby marked "advertisement" in accordance with 18 USC section 1734. This study was supported by a grant-in-aid from the Ministry of Education, Science and Culture of Japan (21390400 and 23390342) and by the "Project for Developing Innovation Systems" from the Ministry of Education, Culture, Sports, Science and Technology, the Japanese government. No other potential conflict of interest relevant to this article was reported.

REFERENCES

1. Azizi SA, Stokes D, Augelli BJ, DiGirolamo C, Prockop DJ. Engraftment and migration of human bone marrow stromal cells implanted in the brains of albino rats: similarities to astrocyte grafts. *Proc Natl Acad Sci USA*. 1998;95:3908–3913.
2. Kopen GC, Prockop DJ, Phinney DG. Marrow stromal cells migrate throughout forebrain and cerebellum, and they differentiate into astrocytes after injection into neonatal mouse brains. *Proc Natl Acad Sci USA*. 1999;96:10711–10716.
3. Sanchez-Ramos J, Song S, Cardozo-Pelaez F, et al. Adult bone marrow stromal cells differentiate into neural cells in vitro. *Exp Neurol*. 2000;164:247–256.
4. Woodbury D, Schwarz EJ, Prockop DJ, Black IB. Adult rat and human bone marrow stromal cells differentiate into neurons. *J Neurosci Res*. 2000;61:364–370.
5. Zhong C, Qin Z, Zhong CJ, Wang Y, Shen XY. Neuroprotective effects of bone marrow stromal cells on rat organotypic hippocampal slice culture model of cerebral ischemia. *Neurosci Lett*. 2003;342:93–96.
6. Neuhuber B, Timothy Himes B, Shumsky JS, Gallo G, Fischer I. Axon growth and recovery of function supported by human bone marrow stromal cells in the injured spinal cord exhibit donor variations. *Brain Res*. 2005;1035:73–85.
7. Hokari M, Kuroda S, Shichinohe H, Yano S, Hida K, Iwasaki Y. Bone marrow stromal cells protect and repair damaged neurons through multiple mechanisms. *J Neurosci Res*. 2008;86:1024–1035.
8. Shichinohe H, Kuroda S, Tsuji S, et al. Bone marrow stromal cells promote neurite extension in organotypic spinal cord slice: significance for cell transplantation therapy. *Neurorehabil Neural Repair*. 2008;22:447–457.
9. Choumerianou DM, Dimitriou H, Perdikogianni C, Martimianaki G, Riminucci M, Kalmanti M. Study of oncogenic transformation in ex vivo expanded mesenchymal cells, from paediatric bone marrow. *Cell Prolif*. 2008;41:909–922.
10. Kuroda S, Shichinohe H, Houkin K, Iwasaki Y. Autologous bone marrow stromal cell transplantation for central nervous system disorders: recent progress and perspective for clinical application. *J Stem Cells Regen Med*. 2011;7:2–13.
11. Savitz SI, Chopp M, Deans R, Carmichael ST, Phinney D, Wechsler L. Stem cell therapy as an emerging paradigm for stroke (STEPS) II. *Stroke*. 2011;42:825–829.
12. The STEPS Participants. Stem cell therapies as an emerging paradigm in stroke (STEPS): bridging basic and clinical science for cellular and neurogenic factor therapy in treating stroke. *Stroke*. 2009;40:510–515.
13. Abe K, Yamashita T, Takizawa S, Kuroda S, Kinouchi H, Kawahara N. Stem cell therapy for cerebral ischemia: from basic science to clinical applications. *J Cereb Blood Flow Metab*. 2012;32:1317–1331.

14. Sugiyama T, Kuroda S, Osanai T, et al. Near-infrared fluorescence labeling allows noninvasive tracking of bone marrow stromal cells transplanted into rat infarct brain. *Neurosurgery*. 2011;68:1036–1047, discussion 1047.
15. Hoehn M, Kustermann E, Blunk J, et al. Monitoring of implanted stem cell migration in vivo: a highly resolved in vivo magnetic resonance imaging investigation of experimental stroke in rat. *Proc Natl Acad Sci USA*. 2002;99:16267–16272.
16. Jendelová P, Herynek V, DeCros J, et al. Imaging the fate of implanted bone marrow stromal cells labeled with superparamagnetic nanoparticles. *Magn Reson Med*. 2003;50:767–776.
17. Modo M, Mellodew K, Cash D, et al. Mapping transplanted stem cell migration after a stroke: a serial, in vivo magnetic resonance imaging study. *Neuroimage*. 2004;21:311–317.
18. Ito M, Kuroda S, Sugiyama T, et al. Validity of bone marrow stromal cell expansion by animal serum-free medium for cell transplantation therapy of cerebral infarct in rats: a serial MRI study. *Transl Stroke Res*. 2011;2:294–306.
19. Mori K, Iwata J, Miyazaki M, Nakao Y, Maeda M. Functional recovery of neuronal activity in rat whisker-barrel cortex sensory pathway from freezing injury after transplantation of adult bone marrow stromal cells. *J Cereb Blood Flow Metab*. 2005;25:887–898.
20. Shichinohe H, Kuroda S, Yano S, et al. Improved expression of gamma-aminobutyric acid receptor in mice with cerebral infarct and transplanted bone marrow stromal cells: an autoradiographic and histologic analysis. *J Nucl Med*. 2006;47:486–491.
21. Yano S, Kuroda S, Shichinohe H, et al. Bone marrow stromal cell transplantation preserves gammaaminobutyric acid receptor function in the injured spinal cord. *J Neurotrauma*. 2006;23:1682–1692.
22. Kawabori M, Kuroda S, Sugiyama T, et al. Intracerebral, but not intravenous, transplantation of bone marrow stromal cells enhances functional recovery in rat cerebral infarct: an optical imaging study. *Neuropathology*. 2012;32:217–226.
23. Sugiyama T, Kuroda S, Takeda Y, et al. Therapeutic impact of human bone marrow stromal cells expanded by animal serum-free medium for cerebral infarct in rats. *Neurosurgery*. 2011;68:1733–1742.
24. Bederson JB, Pitts LH, Tsuji M, Nishimura MC, Davis RL, Bartkowski H. Rat middle cerebral artery occlusion: evaluation of the model and development of a neurologic examination. *Stroke*. 1986;17:472–476.
25. Yano S, Kuroda S, Shichinohe H, Hida K, Iwasaki Y. Do bone marrow stromal cells proliferate after transplantation into mice cerebral infarct? A double labeling study. *Brain Res*. 2005;1065:60–67.
26. Rustay NR, Wahlsten D, Crabbe JC. Assessment of genetic susceptibility to ethanol intoxication in mice. *Proc Natl Acad Sci USA*. 2003;100:2917–2922.
27. Kemp BJ, Hruska CB, McFarland AR, Lenox MW, Lowe VJ. NEMA NU 2-2007 performance measurements of the Siemens Inveon preclinical small animal PET system. *Phys Med Biol*. 2009;54:2359–2376.
28. Magota K, Kubo N, Kuge Y, Nishijima K, Zhao S, Tamaki N. Performance characterization of the Inveon preclinical small-animal PET/SPECT/CT system for multimodality imaging. *Eur J Nucl Med Mol Imaging*. 2011;38:742–752.
29. Visser EP, Disselhorst JA, Brom M, et al. Spatial resolution and sensitivity of the Inveon small-animal PET scanner. *J Nucl Med*. 2009;50:139–147.
30. Disselhorst JA, Brom M, Laverman P, et al. Image-quality assessment for several positron emitters using the NEMA NU 4-2008 standards in the Siemens Inveon small-animal PET scanner. *J Nucl Med*. 2010;51:610–617.
31. Locke LW, Berr SS, Kundu BK. Image-derived input function from cardiac gated maximum a posteriori reconstructed PET images in mice. *Mol Imaging Biol*. 2011;13:342–347.
32. Ito M, Kuroda S, Sugiyama T, et al. Transplanted bone marrow stromal cells protect neurovascular units and ameliorate brain damage in stroke-prone hypertensive rats. *Neuropathology*. 2012;32:522–533.
33. Moore AH, Osteen CL, Chatziioannou AF, Hovda DA, Cherry SR. Quantitative assessment of longitudinal metabolic changes in vivo after traumatic brain injury in the adult rat using FDG-microPET. *J Cereb Blood Flow Metab*. 2000;20:1492–1501.
34. Shimoji K, Ravasi L, Schmidt K, et al. Measurement of cerebral glucose metabolic rates in the anesthetized rat by dynamic scanning with ¹⁸F-FDG, the ATLAS small animal PET scanner, and arterial blood sampling. *J Nucl Med*. 2004;45:665–672.
35. Mori K, Schmidt K, Jay T, et al. Optimal duration of experimental period in measurement of local cerebral glucose utilization with the deoxyglucose method. *J Neurochem*. 1990;54:307–319.
36. Wood IS, Trayhurn P. Glucose transporters (GLUT and SGLT): expanded families of sugar transport proteins. *Br J Nutr*. 2003;89:3–9.
37. Vannucci SJ, Reinhart R, Maher F, et al. Alterations in GLUT1 and GLUT3 glucose transporter gene expression following unilateral hypoxia-ischemia in the immature rat brain. *Brain Res Dev Brain Res*. 1998;107:255–264.
38. Zhang WW, Zhang L, Hou WK, et al. Dynamic expression of glucose transporters 1 and 3 in the brain of diabetic rats with cerebral ischemia reperfusion. *Chin Med J (Engl)*. 2009;122:1996–2001.
39. Espinoza-Rojo M, Iturralde-Rodriguez KI, Chanez-Cardenas ME, Ruiz-Tachiquin ME, Aguilera P. Glucose transporters regulation on ischemic brain: possible role as therapeutic target. *Cent Nerv Syst Agents Med Chem*. 2010;10:317–325.



The Journal of
NUCLEAR MEDICINE

Bone Marrow Stromal Cell Transplantation Enhances Recovery of Local Glucose Metabolism After Cerebral Infarction in Rats: A Serial ^{18}F -FDG PET Study

Michiyuki Miyamoto, Satoshi Kuroda, Songji Zhao, Keiichi Magota, Hideo Shichinohe, Kiyohiro Houkin, Yuji Kuge and Nagara Tamaki

J Nucl Med. 2013;54:145-150.

Published online: November 30, 2012.

Doi: 10.2967/jnumed.112.109017

This article and updated information are available at:

<http://jnm.snmjournals.org/content/54/1/145>

Information about reproducing figures, tables, or other portions of this article can be found online at:

<http://jnm.snmjournals.org/site/misc/permission.xhtml>

Information about subscriptions to JNM can be found at:

<http://jnm.snmjournals.org/site/subscriptions/online.xhtml>

The Journal of Nuclear Medicine is published monthly.
SNMMI | Society of Nuclear Medicine and Molecular Imaging
1850 Samuel Morse Drive, Reston, VA 20190.
(Print ISSN: 0161-5505, Online ISSN: 2159-662X)

© Copyright 2013 SNMMI; all rights reserved.

 SOCIETY OF
NUCLEAR MEDICINE
AND MOLECULAR IMAGING